Geotechnical Engineering Journal of SEAGS & AGSSEA

https://ph01.tci-thaijo.org/index.php/seags_agssea_journal

# Flexural Strength Properties of Compacted Cement - Fly Ash from Municipal Solid Waste - Polypropylene Fiber Sand

Wungsumpow C.[1], Pochalard S.[2], Bardet K.[3], and Piriyakul K.[4, *]

[1] *KMUTNB Techno Park, King Mongkut's University of Technology North Bangkok, Thailand*

[2] *Building and Landscape Division, Suan Dusit University, Bangkok, Thailand*

[3] *CESI Nanterre École d'Ingénieurs (CESI Engineering School), Nanterre, France*

[4, *] *Center of Excellence in Structural Dynamics and Urban Management, Science and Technology Research Institute, and Department of Civil and Environmental Engineering Technology, College of Industrial Technology, King Mongkut's University of Technology North Bangkok, Bangkok, Thailand*

*E-mail: keeratikan.p@cit.kmutnb.ac.th*

**ABSTRACT:** This research aims to enhance the flexural strength of cement compacted sand using fly ash from municipal solid waste (MSW) and polypropylene fiber (CCFFS). This MSW combustor fly ash is the by-product and is produced during the combustion of municipal solid waste in solid waste combustor facilities. Incineration has overtaken landfill mining as the most important option for disposal of the increasing volumes of MSW generated in Thailand. The research purposes this new green material (CCFFS) and studies its properties which are first peak strength, peak strength, peak strength ratio, toughness, ductility index, equivalent flexural strength and crack behavior. The CCFFS samples were prepared by adding 5% of cement by weight, varying the fly ash replacement to cement ratio of 0:100, 25:75, 50:50, 75:25 and 100:0 by weight, and varied polypropylene fiber of 0, 0.5, 1, 1.5 and 2% by volume. Then all CCFFS samples were cured for 28 days to reach their maximum capacity. From the results, the research recommends the fly ash replacement to cement ratio of 25:75 and the polypropylene fiber of 1.5% by volume showing the maximum flexural strength. The polypropylene fiber under investigation has a non-compact interfacial zone that SEM results in only a partial-contact interfacial surface, making them hydrophobic materials. These need to form a strong enough bond with a higher fiber content to produce a hardening-deflection response. The CCFFS has been proven to be a sustainable construction material. These support Thailand's future cement demand while lowering the cement industry's greenhouse gas emissions.

**KEYWORDS:** Flexural Strength, Municipal Solid Waste (MSW), Fly Ash, Polypropylene Fiber, and Cement Compacted Sand.

## 1. INTRODUCTION

Natural resources are depleted, and the environment is harmed by the large-scale material extraction needed for conventional construction and building materials, including steel bars, cement, concrete, sandcrete blocks, burned bricks, and tiles. The production process for these materials is energy demanding, releasing carbon dioxide and other pollutants into the environment, such as particulate matter, sulfur oxides, nitrogen oxides, and carbon monoxide. These pollutants contaminate water, air, soil, vegetation, wildlife, and aquatic life, and also impact human health (Safiuddin et al., 2010). Furthermore, the cost of traditional building materials continues to rise due to the energy required for manufacturing, scarcity of natural resources, and high transportation costs from manufacturers to construction sites. These environmental and economic concerns have sparked interest in research into alternative building materials (Danso et al., 2015). Earth material requires about 99% less energy during production than industrial building materials like concrete. Long transportation routes are also superfluous because earth is a locally accessible, affordable, and recyclable building material (Zak et al., 2016). Because of its low cost and minimal environmental impact, the use of earth as a construction material for producing rammed earth is gaining popularity (Sharma et al., 2015). However, in terms of durability, tensile strength, and compressive strength, earthen materials are not as strong as modern building materials such as steel and concrete (Ngowi, 1997). Cement is frequently used in these stabilizers to increase the strength characteristics of the soil. Cement, however, is just one of several factors contributing to the indicated $CO_2$ emissions (Safiuddin et al., 2010; Ayeldeen & Kitazume, 2017). Consequently, there has been increased focus on fiber-reinforced cementitious soil to improve the mechanical properties of the soil (Ayeldeen & Kitazume, 2017; Consoli et al., 2010; Xiao & Liu, 2018; Tran et al., 2017). Because it softens and can undergo plastic deformation when heated gradually, polyethylene (PE) is a lightweight, viscoelastic, and thermoplastic material. It returns to its hard state upon cooling. The average chain length determines the temperature at which this occurs (Elmrabet et al., 2020). As a result, concrete with a Fly Ash from Municipal Solid Waste (MSWIFA) blend, used as a substitute for building materials, reduces environmental costs, including $CO_2$ emissions, by eliminating cement, while also providing a location for MSWIFA to develop (currently stored in old mines) (Poranek, 2023). These wastes are part of landfill mining. In general, Landfill mining is the excavation and processing of landfilled waste to produce recyclable materials, soil-like material, and refuse-derived fuel (RDF). Effective landfill mining necessitates systematic planning. (Wungsumpow et al., 2018). MSWIFA can be used as a sustainable construction material. It is one of the sustainable materials, as reviewed by Al-Ghouti et al. (2021), so it is important to understand the introduction and background, the experimentation, the results, and the expected benefits of this study. For the introduction and background, Bellum (2022) studied the mechanical properties of cement mortars incorporating fly ash from industry and Ground Granulated Blast-Furnace Slag (GGBFS), with polypropylene fiber.

Fibers are used to improve the tensile behavior of construction building materials. Much research has used cementitious materials and fibers in their work for many decades; for example, Iamchaturapatr et al. (2022a), Iamchaturapatr et al. (2022b), Yingsamphancharoen & Piriyakul (2022), and Petcherdchoo et al.

https://doi.org/10.14456/seagj.2026.1 Published on 24 June 2026

(2023). A group of soil engineers (Pochalard et al., 2024) developed a new eco-friendly functional road material which is made of Bangkok clay, cement, bottom ash from the Refuse Derived Fuel (RDF) power plant, and glass fibers. By using the unconfined compression test (UCS), all samples were mixed at the liquid limit (LL) of 88%, varying glass fiber content between 0.5, 1.0, 1.5, 2.0, and 2.5% by volume, respectively, and the glass fiber lengths of 3, 6, and 12 mm. The cement content is used between 2, 4, 6, 8, and 10%, respectively, by dry weight. The bottom ash (BA) content is used at 5%, 10%, 15%, 20%, 25%, and 30% by volume. Then, the tested samples are cured for 7, 14, 28, 60, and 90 days. From the test results, it was observed that the optimum cement content is 8 to10% according to ACI 230.1R-09 standard, which requires OPC of 10 to16%, and the optimum glass fiber content is between 1.0 and 1.5%. The best UCS result for glass fiber length is at 12 mm. Finally, the optimum bottom ash content is 5 to10%, and the curing time should go beyond 28-90 days. A group of civil engineers (Pochalard et al., 2024) studied the influence of novel high-strength polyethylene fibers on the unconfined compressive strength (UCS) behavior of Bangkok clay cement admixed. Bangkok clay samples are prepared at a liquid limit (LL) of 88% and added to Ordinary Portland Cement (OPC) at 2, 4, 6, 8, and 10% by weight; polyethylene fibers are added at 0.5, 1.0, 1.5, 2.0, and 2.5% by volume. These Bangkok clay samples are cured for 7, 14, and 28 days and tested by the unconfined compressive test. From the test results, it was found that a cement content of 8% by weight is the optimum, and a novel high-strength polyethylene fiber content of 1% by volume is recommended. Additionally, the novel high-strength polyethylene fiber with a diameter of 0.2 mm and a length of 6 mm resulted in the maximum UCS value. A group of geotechnical engineers (Wungsumpow et al., 2024) investigates the strength development of Bangkok clay mixed with cement and Fly Ash (FA) from an RDF power plant. The cement is replaced with FA, an eco-friendly approach since it is an industrial waste product from the Mae Moh power plant in northern Thailand. Bangkok clay is mixed with 20% cement by weight, with FA varying from 0 to 30% by weight, after curing for 7, 14, 28, and 90 days. The initial shear modulus ($G_0$) is calculated from the shear wave velocity ($V_s$) measured by a bender element test. For comparison, the strength development of Bangkok clay samples is determined using the unconfined compression test (UCS). From the results, it was noted that the optimum FA content is about 15-20%, and it was established that the strength development of Bangkok clay admixed with cement and FA increases with increasing curing time. Furthermore, the relationship is given by $G_0=27.57q_u$.

The use of fly ash from MSW is an interesting topic in environmental management in Thailand, so this study enhances the flexural strength of Cement Compacted Sand using Fly Ash from MSW and Polypropylene Fiber (CCFFS) to investigate its environmental benefits. MSW combustor fly ash is the by-product that is created when municipal solid waste is burned in solid waste combustor plants, which is known as MSW combustor fly ash (Chesner et al., 2002). Incineration has surpassed landfill mining as the most significant alternative for disposing of Thailand's growing amounts of waste (Wang et al., 2019). The sand examined came from Thailand's Ayutthaya area and is often utilized as a building material for embankment fill and pavement applications (Chuenjaidee et al., 2022). As a cementing agent, type I Portland cement was employed with fly ash from MSW (Aubert et al., 2004), and polypropylene fibers were used as reinforcement material (Blazy & Blazy, 2021). Water was added to the CCFFS mixture to achieve the optimal water content as determined by the standard Proctor test ASTM D698-12e1 (ASTM, 2009). The experimentation involves research on the properties of the CCFFS according to ASTM C 1018 (1997) and ASTM C-09 (2013), and the objective of this investigation is to study unconfined compressive tests by adding polyethylene, with variations in fiber content, cement content, and curing time. Thus, the CCFFS performance was examined, including first peak strength, peak strength, peak strength ratio, toughness, ductility index, equivalent flexural strength, and crack behavior (Jamsawang et al., 2015).

According to the aforementioned literature reviews, there are two issues to be further addressed. First, the application of fly ash from the RDF power plant to replace the ordinary Portland cement (OPC) based on the flexural test. Second, the microstructure and bonding between the polypropylene fiber and soil matrix were examined using SEM.

## 2. EXPERIMENTATION

The experimentation was divided into three sections. First, the geotechnical properties of the examined sand, as well as the physical and engineering features of fiber and fly ash from MSW. There are physical property tests of the Bangkok construction sand, including Specific gravity ($G_s$), Gravel content, Sand content, Fine content, $D_{60}$, $D_{30}$, $D_{10}$, Coefficient of Uniformity ($C_u$), Coefficient of Curvature ($C_c$), Coefficient of Curvature ($C_c$), Maximum and minimum void ratios, Maximum dry unit weight, Optimum moisture content, and Optimum moisture content. The chemical composition, using an X-ray fluorescence spectrometer (XRF) testing, of the ordinary portland cement (OPC) includes silica, Alumina, Iron, Sulfuric anhydrite, Lime, Magnesia, Alkali, Chromium oxide, and Zinc oxide. The properties of polypropylene fiber include length, shape, section, diameter, specific weight, tensile strength, Young's modulus, and Colour. The chemical composition of RDF fly ash includes percentages by mass of silica, Alumina, Iron, Sulfuric Anhydride, Lime, Magnesia, Alkali, chromium oxide, and Zinc oxide. Second, the CCFFS specimens were subjected to a series of flexural strength tests using a 50 kN load cell to measure the applied loads. The deflection rate was controlled by an electric motor at 0.05 mm/min, and the test ended after a net deflection of 3 mm. The CCFFS specimens were made by mixing dry Bangkok sand, fly ash from municipal solid waste (MSW), polypropylene fibers, and Portland cement in a concrete mixer. And, CCFFS specimens were prepared as a beam measuring 75 mm in width, 75 mm in height, and 300 mm in length. Last, a series of scanning electron microscope (SEM): FEI QUANTA 450 investigations were performed on the CCFFS samples to examine the interaction mechanism of fiber, cement, and fly ash from MSW interface and to explain the influence of fiber on the flexural performances of the CCFFS specimens test beam for the purpose of determining an appropriate material ratio as shown in Figure 2.

### 2.1 Materials

Sand used in the current experiments was the typical Bangkok construction sand. The grain size analysis curve and physical properties of Bangkok sand are shown in Figure 1 and Table 1, respectively. According to the Unified Soil Classification System (USCS), this Bangkok sand is classed as poorly graded sand (SP). Figure 3 also shows an enlargement of the sand particles obtained from the SEM image analysis, which shows angular, sub-angular, round, and sub-round shapes. Figure 4 depicts the modified proctor curve of Bangkok sand. It was found that the maximum dry density is 17 kN/m$^3$ and the optimum moisture content is 6.19 %. Ordinary Portland cement type I, with a specific gravity of 3.15, was used in the test. The chemical composition of the cement used is summarized in Table 2. The fibers used in this experiment were macro polypropylene fibers, and the size is 55 mm, as shown in Figure 5 and Table 3.

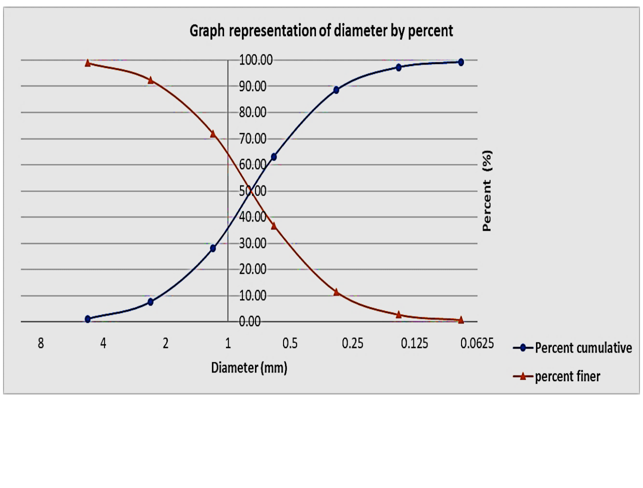

**Figure 1 Grain size distribution curve of Bangkok sand**

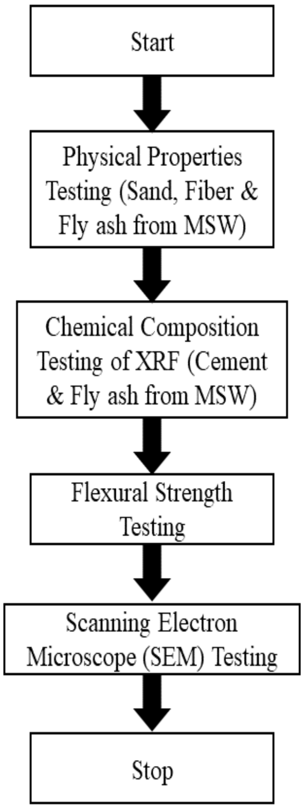


**Figure 2 Flow chart for experimentation**

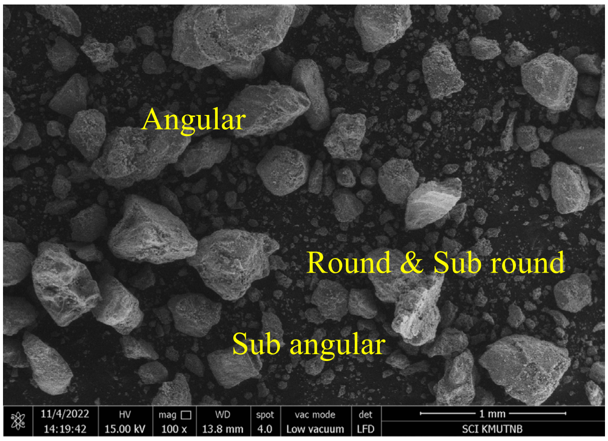


**Figure 3 SEM image of Bangkok construction sand**

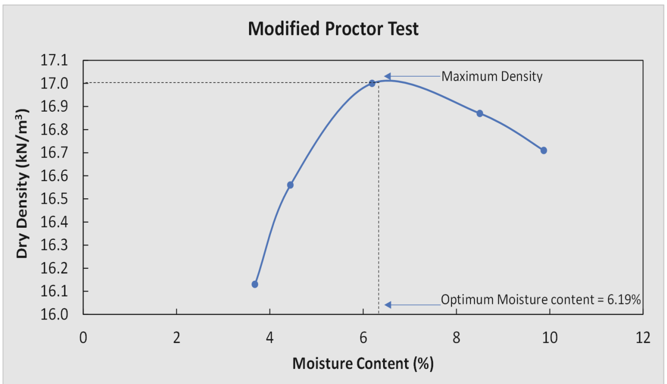


**Figure 4 Modified proctor curve of Bangkok sand**

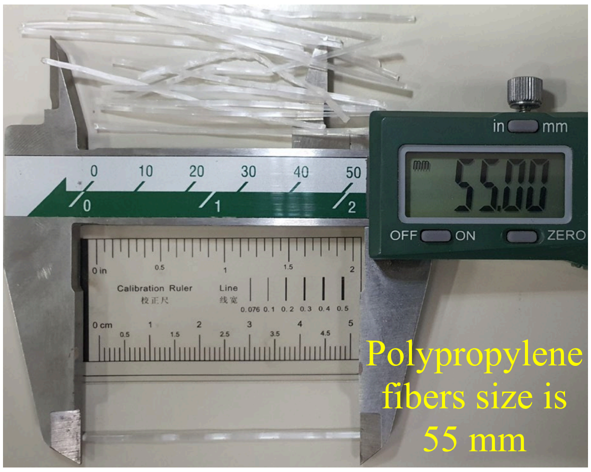


**Figure 5 Polypropylene fibers**

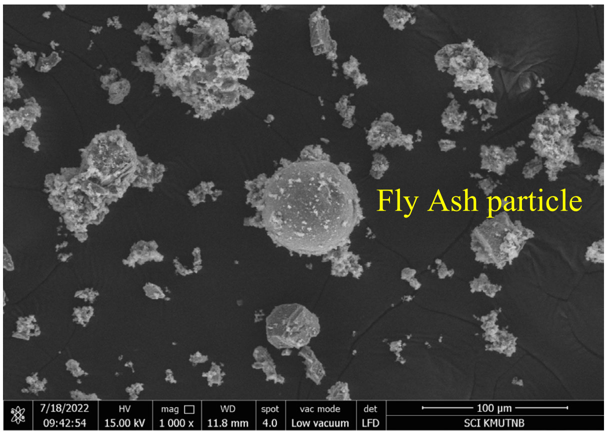


**Figure 6 SEM image of fly ash from MSW**

**Table 1 Physical properties of the Bangkok construction sand**

| **Property** | **Value** |
|---|---|
| Specific gravity ($G_s$) | 2.65 |
| Gravel content (%) | 10.52 |
| Sand content (%) | 80.58 |
| Fine content (%) | 8.90 |
| $D_{60}$ (mm) | 0.93 |
| $D_{30}$ (mm) | 0.49 |
| $D_{10}$ (mm) | 0.29 |
| Coefficient of Uniformity ($C_u$) | 3.21 |
| Coefficient of Curvature ($C_c$) | 0.89 |
| Soil classification (USCS) | SP |
| Maximum, and minimum void ratios | 0.83, 0.28 |
| Maximum dry unit weight (kN/m$^3$) | 15.70 |
| Optimum moisture content (%) | 6.19 |

**Table 2 Chemical composition of the cement**

| **Oxide** | **Common name** | **Mass (%)** |
|---|---|---|
| $SiO_2$ | Silica | 4.45 |
| $Al_2O_3$ | Alumina | 1.31 |
| $Fe_2O_3$ | Iron | 14.37 |
| $SO_3$ | Sulfuric anhydrite | 1.00 |
| CaO | Lime | 76.44 |
| MgO | Magnesia | 1.79 |
| $K_2O$ | Alkali | 0.23 |
| $Cr_2O_3$ | Chromic oxide | 0.10 |
| ZnO | Zinc oxide | 0.32 |

**Table 3 Properties of polypropylene fiber**

| **Type** | **Polypropylene** |
|---|---|
| Length (mm) | 55 |
| Shape | Crimped |
| Section | Circular |
| Diameter (mm) | 0.85 |
| Specific weight | 0.91 |
| Tensile strength (MPa) | 250 |
| Young's modulus (GPa) | 3.0 |
| Colour | White |

**Table 4 Chemical composition of the RDF fly (Fly ash from MSW)**

| **Oxide** | **Common name** | **Mass (%)** |
|---|---|---|
| $SiO_2$ | Silica | 4.45 |
| $Al_2O_3$ | Alumina | 1.31 |
| $Fe_2O_3$ | Iron | 14.37 |
| $SO_3$ | Sulfuric anhydrite | 1.00 |
| CaO | Lime | 76.44 |
| MgO | Magnesia | 1.79 |
| $K_2O$ | Alkali | 0.23 |
| $Cr_2O_3$ | Chromic oxide | 0.10 |
| ZnO | Zinc oxide | 0.32 |

## 2.3 Experimentation

The specimens performed a flexural performance test in accordance with ASTM C 1018 (1997) and ASTM C-09 (2013) after 28 days of curing. The beams were turned 90 degrees from their casting location before testing to reduce the impact of the casting direction. The test setup and equipment are displayed in Figures 7 and 8. The applied loads were measured using a 50 kN load cell. An electric motor controlled the deflection rate of 0.05 mm/min, and the test ended at a net deflection of 3 mm. Then, the data logger then gathered enough data points to create highly sensitive load-deflection curves as seen in Figure 9, which were then utilized to accurately predict each CCFFS's dependable flexural performance and interpret the test findings.

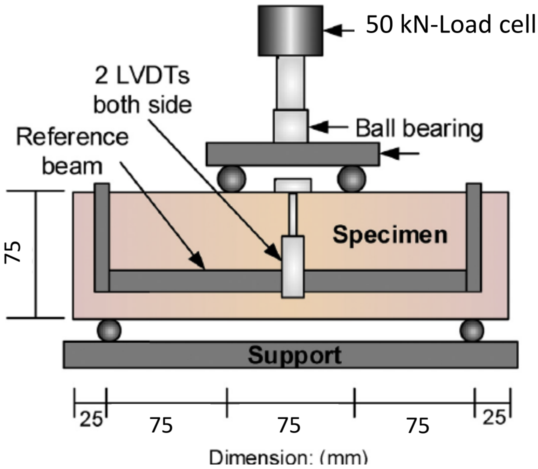


**Figure 7 Test specimen and set up**

## 2.4 The CCFFS's flexural behavior parameters

The CCFFS flexural responses can be classified as softening or hardening. Figure 9 shows the load-deflection curves for CCFFS beams. Beams with no fiber have deflection softening and brittle behavior, while beams containing a lot of fibers show deflection hardening and ductile behavior. Flexural reactions of CCFFS can be characterized as either deflection-softening or deflection-hardening, as illustrated by the curves. In this study, along the load-deflection curve, the point that clearly shows nonlinearity is defined as the first cracking point. After initial cracking, a CCFFS sample exhibiting deflection-hardening behavior has a higher load-carrying capacity. According to ASTM C 1018 (1997) and ASTM C-09 (2013), this point is suitable for designating the first peak point for CCFFSs displaying either deflection-hardening or softening reactions. $P_1$ is the load value at this point, and $\delta_1$ is a corresponding deflection value. The first softening point following point P1 is known as the peak load (PP). In the case of deflection-softening CCFFS, it is observed that P1 = PP. δP denotes the corresponding deflection value at PP. ASTM C-09 (2013) recommends a deflection point at L/150, equivalent to 1.5 mm, for a specimen with a 1.5 mm span, in addition to the $P_1$ and $P_P$ points. At any deflection, the flexural strength (f) is calculated by Eq. (1) as follows:

$$f = \frac{PL}{bd^2} \tag{1}$$

P is the load (kN) that corresponds to the needed f (kPa), L is the span length (m), b is the specimen's breadth (m), and d is its depth (m). The $P_1$ and $P_P$ flexural loads are defined as the first peak strength ($f_1$) and the peak strength ($f_P$). The residual load $P_{150}$, which equates to the residual strength at a deflection of L/150 ($f_{150}$), is the load borne by CCFFS after $P_1$ at the deflection of L/150. Toughness is defined as the energy corresponding to the region beneath the load-deflection curve up to a specific deflection. The toughness value at the deflection of L/150 is indicated as $T_{150}$. Nematollahi et al. (2014) state that the ductility of a composite material is defined as the ratio of the first-crack deflection to the deflection at the peak strength ($\delta_P/\delta_1$).

In other words, the CCFFS is more ductile as the ratio of δP/δ1 increases. Thus, the following definition applies to the ductility index (DI) by Eq. (2) as below:

$$DI = \frac{\delta_P}{\delta_1} \quad (2)$$

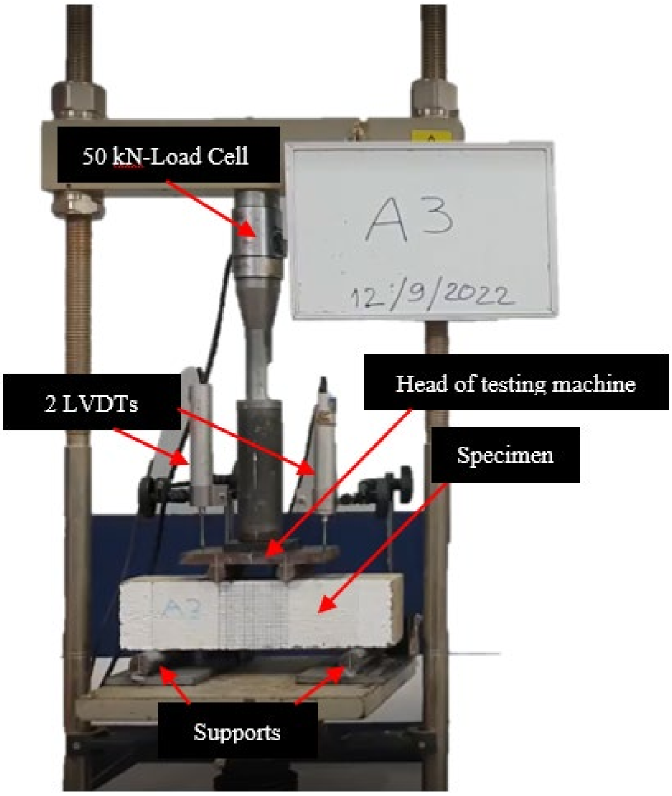


**Figure 8 Setting up the study specimen**

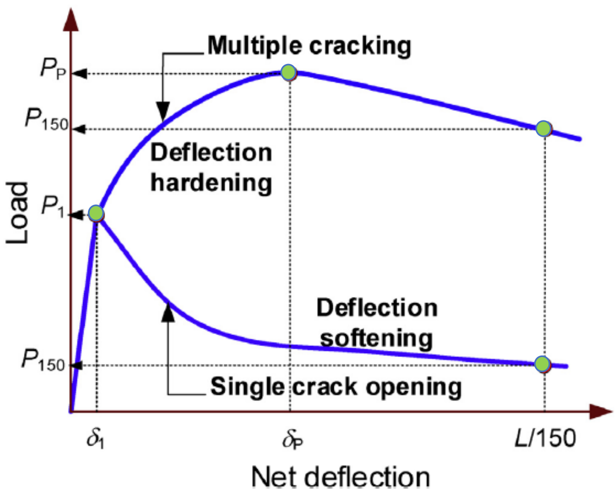


**Figure 9 Parameter calculations obtained from load–deflection curves (adapted from ASTM C1609/C1609M-10, 2010).**

Where $\delta_P$ and $\delta_1$ are the specimen's net deflections at peak strength and first peak strength, in mm. The equivalent flexural strength ratio ($R_{T,150}$), derived from the energy absorption capacity up to a deflection of L/150 of the beam span and the initial peak load, is frequently used to assess the flexural performance of CCFFS. As a result, using Eq. (3), the value of $R_{T,150}$ could be determined from the load deflection curves obtained from the observations.

$$R_{T,150} = \frac{T_{150}}{P_1 \times \left(\frac{L}{150}\right)} \times 100\% \quad (3)$$

A high toughness material is one with an $R_{T,150}$ value greater than 100%, and is linked to $P_P > P_1$. $R_{T,150}$ values, on the other hand, are less than and larger than 100% for deflection softening ($P_P = P_1$) and deflection hardening ($P_P > P_1$) behaviors, correspondingly.

## 2.5 Results and discussions

### 2.5.1 Behavior of load-deflection curves

Figures 10a-e present the load-deflection curves for CCFFS beams with polypropylene fiber contents ranging from 0 to 2.0%. All figures clearly show that fly ash affects the load-deflection response at the same polypropylene fiber content, indicating different flexural performance in terms of first peak strength, peak strength, peak strength ratio, residual strength ratio, ductility index, and toughness. Figure 10a shows the results for CCFFS beams without polypropylene fiber, reflecting brittle behavior and deflection softening. Adding 0.5% polypropylene fiber content improves ductile behavior and increases the residual strength ratio (RSR150) at a deflection of L/150 (Figure 10b). Figure 10c presents the test data of the CCFFS beam mixed with 1% of polypropylene fiber. The test results show that Group B, with 25% fly ash and 75% Portland cement, has $P_{150}$ data as good as those of the controlled Group A, with 100% Portland cement. Figure 10d shows the test results of CCFFS beams with 1.5% of polypropylene fiber. Test data for Group B have $P_{150}$ values higher than the controlled results for Group A, indicating ductile behavior and deflection hardening. However, Figure 10e shows that the test data of the controlled sample group A has deflection hardening behavior and $P_{150}$ data higher than other test results. Therefore, the research found the optimal polypropylene fiber content to be 1.5% for Group B (25% fly ash and 75% cement).

### 2.5.2 First peak strength ($f_1$) and peak strength ($f_P$)

The first crack's stress, or $f_1$, was brought on by bending along the bottom face of the beam. The impact of fiber content on the values of $f_1$ and $f_P$ is depicted in Figures 11 and 12. The CCFFS has $f_1$ values ranging from 0.01 to 0.43 MPa. Because the strength of the cement, sand, and fly ash from the MSW matrix, rather than the fiber bridging capacity, determines f1 for CCFFS, an increase in fiber content has a minor effect (Sukontasukkul et al., 2010). so that all CCFFS, with the exception of CCFFS Group C and CCFFS Group E, which have fiber concentrations ranging from 0.5 to 1.5%, have $f_1$ values that are hardly different from one another. While the fiber content of all CCFFS samples increases, so does the total $f_P$, with the exception of CCFFS Group D and CCFFS Group E.

### 2.5.3 Peak strength ratio (PSR)

Peak strength ratio (PSR), defined as $f_P$ divided by $f_1$, is used in this study to compare the hardening levels of each CCFFS.This ratio shows how strong the fiber can get following the occurrence of the first crack. More specifically, PSR = 1 and PSR > 1 imply responses that alternate between softening and hardening; the greater the PSR, the more hardening has occurred. According to Figure 13, CCFFS Group B and CCFFS Group D showed PSR increases with increasing fiber content, reaching the highest PSRs of 1.1 and 1.86, respectively, at 1.5% and 2.0% fiber content. In contrast, CCFFS Group C and CCFFS Group E showed an optimal fiber concentration of 0.97 with a maximum PSR of around 2.3. As a result, CCFFS Group E has up to 2.45 times the hardness of CCFFS.

Group C and CCFFS Group D (fiber contents 0.5%). With reported values of 1.10 and 1.86, respectively, CCFFS Group B (fiber content 1.5%) and CCFFS Group D (fiber content 2.0%) exhibited PSR better than 1.0 for specified fiber contents. The PSR for fully developed softening in CCFFS Group C, however, was unaffected by fiber content, as it was consistently reported as 1.

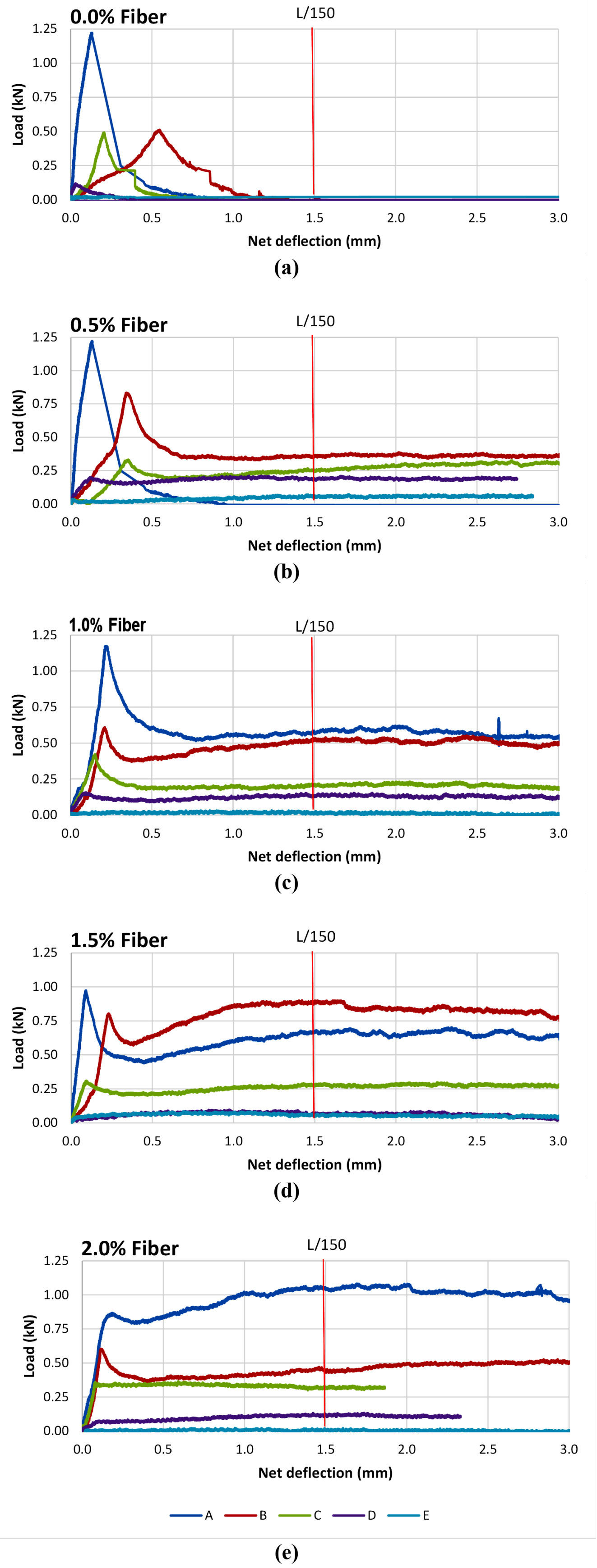


**Figure 10 Load-deflection curves for CCFFS with different fiber contents (a) 0% (b) 0.5% (c) 1.0% (d) 1.5% and (e) 2.0%**

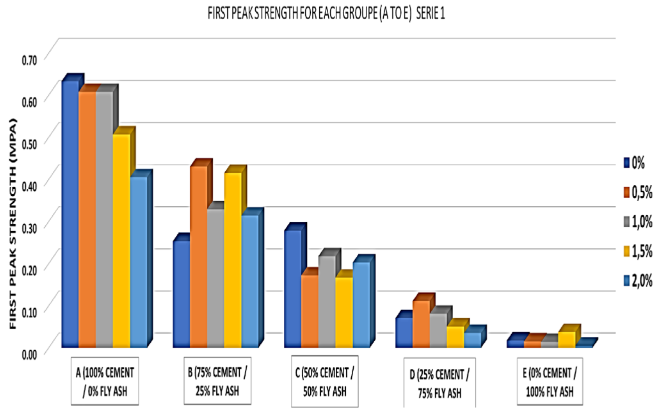


**Figure 11 First peak strength ($f_1$) at different fiber contents and fly ash from WSW replacement to cement ratio**

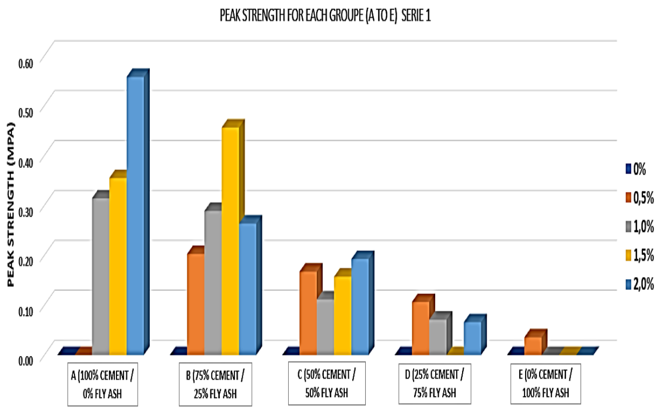


**Figure 12 Peak strength ($f_P$) at different fiber contents and fly ash from WSW replacement to cement ratio**

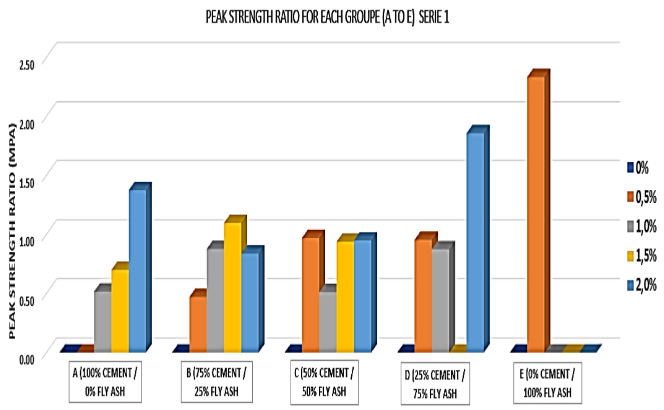


**Figure 13 Peak strength ratio (PSR) at different fiber contents and fly ash from WSW replacement to cement ratio**

### 2.5.4 Residual strength ratio deflection L/150 ($RSR_{150}$)

This research also introduces a residual strength ratio at a deflection of L/150 ($RSR_{150}$) to test the fiber's capacity to support the residual load from the initial fracture site to the deflection of L/150 in addition to PSR. $RSR_{150}$ is therefore equal to $f_{150}$ divided by $f_1$. Additionally, this ratio suggests how well the fiber performs in preserving CCFFS's hardening at high deflection. According to the findings for CCFFS Group B, a fiber concentration of 1.5% is ideal for achieving the highest $RSR_{150}$ values, which is roughly 1.10. But for CCFFS Group A and CCFFS Group D $RSR_{150}$ rose as the fiber content increased, producing the greatest values at 2.0% fiber content for each of 1.38 and 1.71, respectively. Among the various fiber types, it appears that CCFFS Group D was the most successful in terms of $RSR_{150}$

considering the 2.0% fiber content, and CCFFS Group E, which is 0.5% fiber content, as shown in Figure 14.

### 2.5.5 Ductility index (DI)

The data indicate that before the polypropylene fibers can support a portion of the load, a significant amount of deflection is required. For Figure 15, the optimal fiber contents for CCFFS Group A, CCFFS Group C, and CCFFS Group E are 1.5%, and that of CCFFS Group B is 2.0%, with maximum DI values of around 17, 23, 24, and 24.17, respectively. DI values for CCFFS Group C tend to decline and rise with increasing fiber levels, yielding values of 23 to 1 at 0.5-2.0% fiber contents. When creating CCFFS with exceptionally high ductility, CCFFS Group A, CCFFS Group C, and CCFFS Group E at 1.5% fiber content, and CCFFS Group B at 2.0% fiber content are acceptable.

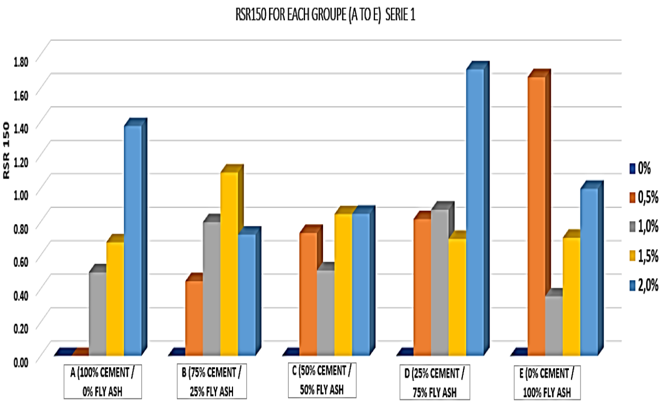


**Figure 14 Residual strength ratio at a deflection of L/150 ($RSR_{150}$) at different fiber contents and fly ash from WSW replacement to cement ratio**

.

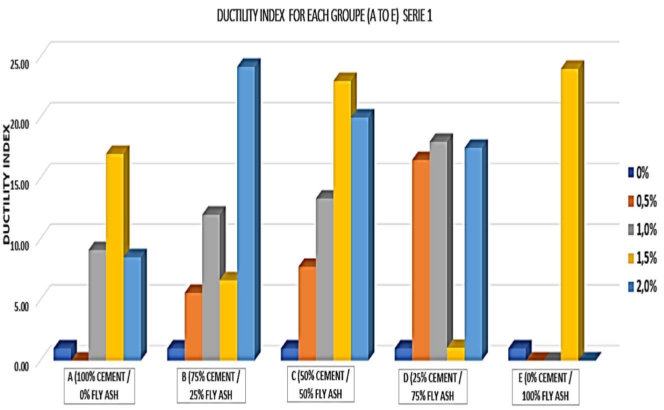


**Figure 15 Ductility index (DI) different fiber contents and fly ash from WSW replacement to cement ratio**

### 2.5.6 Toughness deflection L/150 ($T_{150}$)

This research takes into consideration the toughness at a 1.5 mm deflection point equivalent to L/150 ($T_{150}$). The findings, as shown in Figure 16, demonstrate that the fiber content affects the $T_{150}$ of CCFFS. Because the fiber bridging capacity at the fracture surfaces has improved, higher fiber contents have a higher $T_{150}$. In terms of toughness, CCFFS beams with deflection-hardening behavior outperformed those with deflection-softening behavior because they absorbed more energy following cracking (Hannawi et al., 2016).

As a result, compared with CCFFS with fiber content, CCFFS Group A and CCFFS Group B absorbed the most $T_{150}$, whilst CCFFS Group E produced the least $T_{150}$. $T_{150}$ values from CCFFS Group A and CCFFS Group B ranged from 1.18 to 1.84 N-m and 0.74 to 1.25 N-m, respectively. T150 values from CCFFS Group C, CCFFS Group D, and CCFFS Group E were comparable (between 0.01 and 0.81 N-m). Values between 0.74 and 1.25 N-m were given by CCFFS Group B. $T_{150}$ for CCFFS Group B has a value of 1.25 N-m. Therefore, the CCFFS Group B increased the $T_{150}$ of CCFFS by up to 2.5 and 1.63 times, for the 0.5% and 1.5% fiber content.

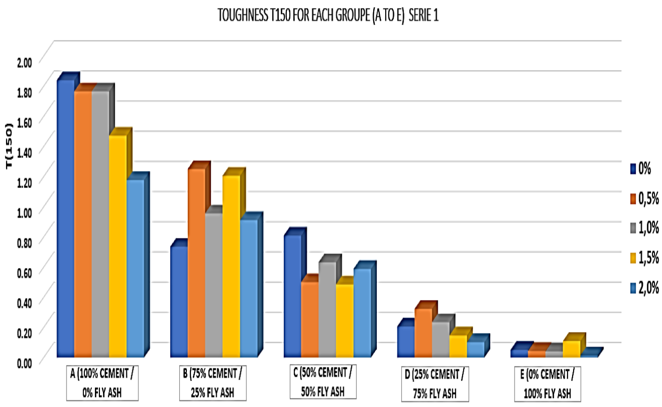


**Figure 16 Toughness at a deflection of L/150 ($T_{150}$) at different fiber contents and fly ash from WSW replacement to cement ratio**

### 2.5.7 SEM image analysis

The effect of fiber type on the crack patterns and crack widths of CCFFS beams. Macroscale crack behavior, which is visible to the unaided eye, is an indication of this study. However, to study the micro-scale interaction mechanisms between the fiber surface micro-scale behavior and the cement-sand matrix interface, microstructural observation is necessary. This intricate process is influenced by various factors, including the shape, surface roughness, and length of the embedded fiber. In order to support the macro-scale test data, it is interesting and reasonable to interpret the comparative flexural performance based on a micromechanical approach as presented in the preceding sections. The comparative interfacial bond nature for the fiber was characterized in this study using SEM observation. The matrix and fiber are first bonded to one another along the whole fiber length by chemical or physical adhesion before the flexural test. According to Hannawi et al. (2016), the SEM images displayed the hydrophobic and synthetic polyolefin and polypropylene fibers. Moreover, SEM analyses verify the presence of $CaCO_3$ binding sand particles together and the enhancement of the physical strength of the sand soil samples (Iamchaturapatr et al., 2021). Furthermore, the use of SEM and an X-ray diffractometer (XRD) to identify the CaCO3 precipitation found in biocemented sand was discussed. Potential benefits and anticipated uses of biocemented soil improvement have been identified (Piriyakul & Iamchaturapatr, 2013). As a result, partially separated interfacial zones were observed because the hydrophobic synthetic fiber was able to more or less prevent the water required for cement hydration from penetrating the structure of the cement sand specimens during the curing period and to increase the number of air bubbles present in the interfacial transition zone. The reduced hardening-deflection response and lower peak strength were caused by this study.

So, the interaction mechanism of fiber-matrix interface is presented by SEM images as shown in Figures 17-21. Figure 17 shows the SEM image of CCFFS in Group A which consists of 100% OPC and no fly ash. The result shows the bonding between the cemented sand matrix and PP fiber due to the hydration reaction. Similarly, Figure 18 shows the SEM image of the sample in Group B, which consists of 75% OPC and 25% fly ash. The hydrophobic zone occurred on the fiber surface, resulting in less bonding and UCS. Moreover, the hydrophobic zone is more pronounced in Group C to Group E since the mixing ratios with fly ash are increased, as shown in Figures 19 – 21. The SEM image of the sample in Group E, which is 100% fly ash and no OPC, shows the severe problem of a hydrophobic zone, showing no bonding on the PP fiber surface and poor UCS results. It was noted that the microstructure of the polypropylene fiber surface, fly ash – cement – sand matrix, hydration products and several interfaces. By adding a small amount of fiber content, the bond strength between the fly ash from the MSW – cement – sand matrix and the polypropylene fiber is created at the polypropylene fiber surface due to hydration products and its crimped-shaped fiber, illustrating the bonding mechanism.

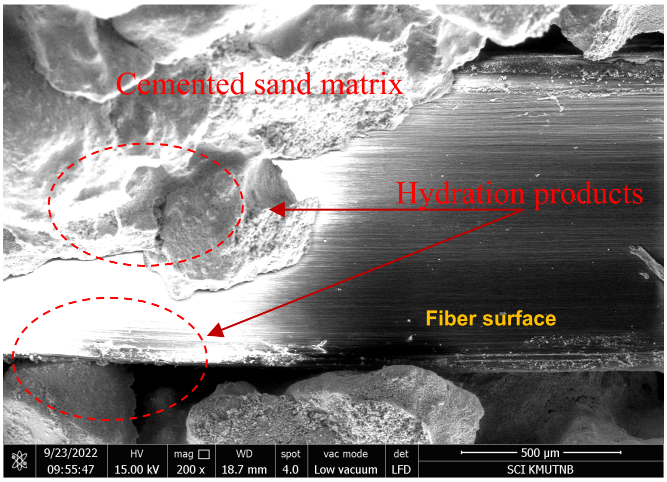


**Figure 17 SEM image of the sample A**

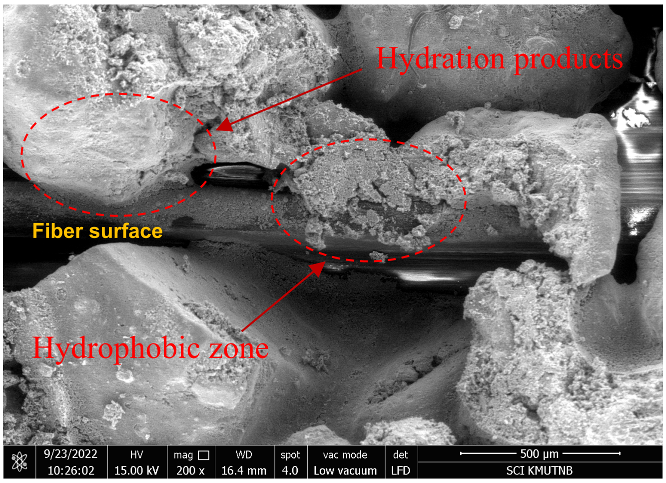


**Figure 18 SEM image of the sample B**

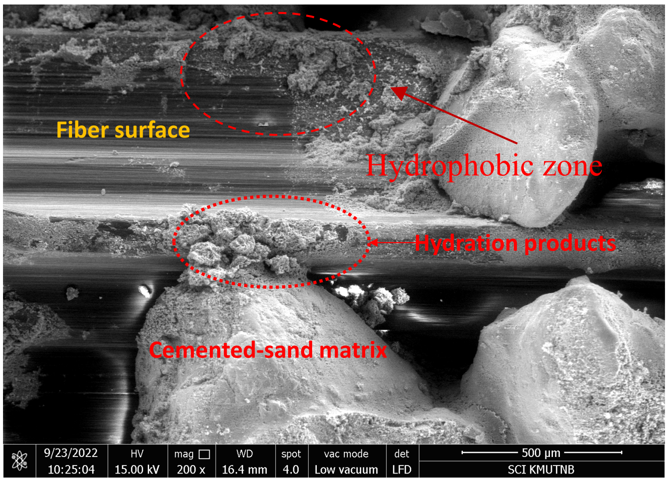


**Figure 19 SEM image of the sample C**

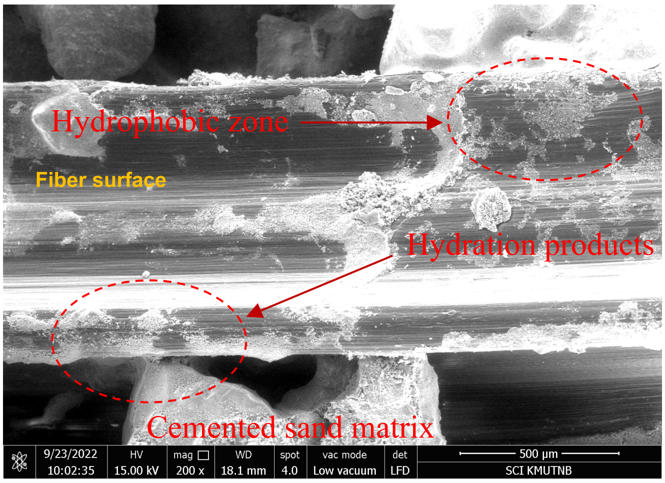


**Figure 20 SEM image of the sample D**

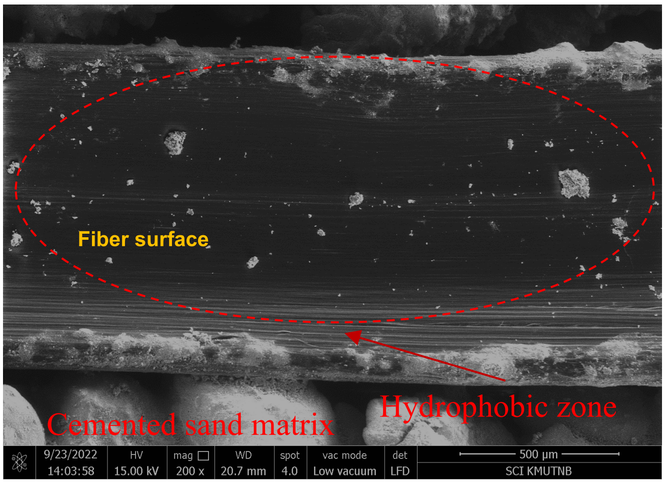


**Figure 21 SEM image of the sample E**

## 3. CONCLUSIONS

This research was conducted as a comparative analysis of the impact of compacted sand using fly ash from MSW and polypropylene fiber (CCFFS) on flexural strength tests, according to ASTM C-1018 (1997) and ASTM C-09 (2013). The cement percentage was set at 5% by dry weight, while the 55 mm polypropylene fiber amounts ranged from 0.5% to 2.0% by volume. And, varying the fly ash replacement to cement ratio of 0:100, 25:75, 50:50, 75:25 and 100:0 by weight. The interaction mechanism of the fiber matrix interface was observed by SEM. Thus, the following conclusions are reached considering the research findings:

1. Fiber composition has an impact on how CCFFS respond to loading. Depending on the amount of fiber present, the CCFFS exhibits either a softening or a hardening reaction. Polypropylene fiber is recommended in terms of achieving a hardening reaction at a fiber content of 1.5%.
2. Fly ash from MSW can be used as a substitute for cement and should not be used at a ratio of more than 25% cement to 75% fly ash for maximum efficiency in the selection of ash materials from MSW.
3. With a non-compact interfacial zone that produces only a partial-contact interfacial surface, the synthetic fibers (polypropylene fiber) under study are hydrophobic materials. For a hardening-deflection response to be obtained, these need a higher fiber content to establish a strong enough bond.
4. More fiber length improves performance for the polypropylene fiber material because it increases the interfacial surface area; however, in the case of differential

lengths, the fiber surface type takes precedence over length because the interfacial bond is different.

5. Polypropylene fiber contributes to the strength of the strengthened sand. The polypropylene fiber worked well to stabilize and reinforce the structure. This is a result of the sand's uniformly distributed fibers.

## 4. ACKNOWLEDGMENTS

This research was funded by National Science, Research and Innovation Fund (NSRF), and King Mongkut's University of Technology North Bangkok with Contract no. KMUTNB-FF-66-33, These financial supports are gratefully acknowledged. King Mongkut's University of Technology North Bangkok and KMUTNB Techno Park, King Mongkut's University of Technology North Bangkok. The authors also extend their appreciation to the CIT and CESI Nanterre École d'Ingénieurs (CESI Engineering School), Nanterre, France for granting staff support through the research collaboration.

## 5. REFERENCES

Al-Ghouti, M. A., Khan, M., Nasser, M. S., Al-Saad, K., & Heng, O. E. (2021). Recent Advances and Applications of Municipal Solid Wastes Bottom and Fly Ashes: Insights into Sustainable Management and Conservation of Resources. Environmental Technology & Innovation, 21, 101267. https://doi.org/10.1016/j.eti.2020.101267

ASTM C1018. (1997). Standard Test Method for Flexural Toughness and First-Crack Strength of Fiber-Reinforced Concrete (Using Beam with Third-Point Loading). Annual Book of ASTM Standards.

ASTM Committee D-18 on Soil and Rock. (2009). Standard Test Methods for Laboratory Compaction Characteristics of Soil Using Modified Effort (56,000 Ft-Lbf/Ft3 (2,700 KN-M/M3)). ASTM International.

ASTM Committee C-09 on Concrete and Concrete Aggregates. (2013). Standard Test Method for Flexural Performance of Fiber-Reinforced Concrete (Using Beam with Third-Point Loading). ASTM International.

Aubert, J. E., Husson, B., & Vaquier, A. (2004). Use of Municipal Solid Waste Incineration Fly Ash in Concrete. Cement and Concrete Research, 34(6), 957–963. https://doi.org/10.1016/j.cemconres.2003.11.002

Ayeldeen, M., & Kitazume, M. (2017). Using Fiber and Liquid Polymer to Improve the Behaviour of Cement-Stabilized Soft Clay. Geotextiles and Geomembranes, 45(6), 592-602.

Bellum, R. R. (2022). Influence of Steel and PP Fibers on Mechanical and Microstructural Properties of Fly Ash-GGBFS Based Geopolymer Composites. Ceramics International, 48(5), 6808–6818. https://doi.org/10.1016/j.ceramint.2021.11.232

Blazy, J., & Blazy, R. (2021). Polypropylene Fiber Reinforced Concrete and Its Application in Creating Architectural Forms of Public Spaces. Case Studies in Construction Materials, 14, e00549. https://doi.org/10.1016/j.cscm.2021.e00549

Chesner, W. H., Collins, R. J., MacKay, M. H., & Emery, J. (2002). User Guidelines for Waste and By-Product Materials in Pavement Construction (No. FHWA-RD-97-148, Guideline Manual, Rept No. 480017). Recycled Materials Resource Center. https://rosap.ntl.bts.gov/view/dot/38365

Chuenjaidee, S., Jamsawang, P., Jongpradist, P., & Chen, X. (2022). Flexural Performance of Cement-Treated Sand Reinforced with Geogrids for Use as Sub-Bases of Pavement and Railway Structures. Materials, 15(8), 2877. https://doi.org/10.3390/ma15082877

Consoli, N. C., Bassani, M. A. A., & Festugato, L. (2010). Effect of Fiber-Reinforcement on the Strength of Cemented Soils. Geotextiles and Geomembranes, 28(4), 344–351.

Danso, H., Martinson, D. B., Ali, M., & Williams, J. (2015). Effect of Fibre Aspect Ratio on Mechanical Properties of Soil Building Blocks. Construction and Building Materials, 83, 314–319.

Elmrabet, R., Elharfi, A., & Elyoubi, M. S. (2020). Study of Properties of Polyethylene and Cement Mixtures. Materials Today: Proceedings, 27, 3017–3020.

Hannawi, K., Bian, H., Prince-Agbodjan, W., & Raghavan, B. (2016). Effect of Different Types of Fibers on the Microstructure and the Mechanical Behavior of Ultra-High-Performance Fiber-Reinforced Concretes. Composites Part B: Engineering, 86, 214–220.

Iamchaturapatr, J., Piriyakul, K., Ketklin, T., Di Emidio, G., & Petcherdchoo, A. (2021). Sandy Soil Improvement Using MICP-Based Urease Enzymatic Acceleration Method Monitored by Real-Time System. Advances in Materials Science and Engineering, 2021, 1–12.

Iamchaturapatr, J., Piriyakul, K., & Petcherdchoo, A. (2022a). Characteristics of Sandy Soil Treated Using EICP-Based Urease Enzymatic Acceleration Method and Natural Hemp Fibers. *Case Studies in Construction Materials*, *16*, e00871.

Iamchaturapatr, J., Piriyakul, K., & Petcherdchoo, A. (2022b). Use of a Piezoelectric Bender Element for the Determination of Initial and Final Setting Times of Metakaolin Geopolymer Pastes, with Applications to Laterite Soils. *Sensors*, *22*(3), 1267.

Jamsawang, P., Voottipruex, P., & Horpibulsuk, S. (2015). Flexural Strength Characteristics of Compacted Cement-Polypropylene Fiber Sand. Journal of Materials in Civil Engineering, 27(9), 04014243.https://doi.org/10.1061/(ASCE)MT.1943-5533.0001205

Nematollahi, B., Sanjayan, J., & Shaikh, F. U. A. (2014). Comparative Deflection Hardening Behavior of Short Fiber Reinforced Geopolymer Composites. Construction and building materials, 70, 54–64.

Petcherdchoo, A., Pochalard, S., & Piriyakul, K. (2023). Use of Bender Element Tests for Determining Shear Modulus of Fly-Ash and Cement Admixed Bangkok Clay with Considering Unconfined Compressive Strength.*Case Studies in Construction Materials*, *18*, e02040.

Piriyakul, K., & Iamchaturapatr, J. (2013). Biocementation through Microbial Calcium Carbonate Precipitation. The Journal of Industrial Technology, 9(3), 195–218.

Pochalard, S., Wungsumpow, C., & Piriyakul, K. (2024). Enhancement of Compressive Strength in Cement Admixed Bangkok Clay with Glass Fiber and Bottom Ash for Eco-Friendly Functional Road Materials. *Mechanics of Advanced Composite Structures*.

Poranek, N., Pizoń, J., Łaźniewska-Piekarczyk, B., Czajkowski, A., & Lagashkin, R. (2023). Recycle Option for Municipal Solid Waste Incineration Fly Ash (MSWIFA) as a Partial Replacement for Cement in Mortars Containing Calcium Sulfoaluminate Cement (CSA) and Portland Cement to Save the Environment and Natural Resources. Materials, 17(1), 39.

Safiuddin, M., Jumaat, M. Z., Salam, M. A., Islam, M. S., & Hashim, R. (2010). Utilization of Solid Wastes in Construction Materials. International Journal of Physical Sciences, 5(13), 1952-1963.

Sharma, V., Vinayak, H. K., & Marwaha, B. M. (2015). Enhancing Compressive Strength of Soil Using Natural Fibers. Construction and Building Materials, 93, 943–949.

Sukontasukkul, P., Pomchiengpin, W., & Songpiriyakij, S. (2010). Post-Crack (or Post-Peak) Flexural Response and Toughness of Fiber Reinforced Concrete after Exposure to High Temperature. Construction and Building Materials, 24(10), 1967-1974.

Tran, K. Q., Satomi, T., & Takahashi, H. (2017). Study on Strength Behavior of Cement Stabilized Sludge Reinforced with Waste Cornsilk Fiber. GEOMATE Journal, 13(39), 140–147.

Wang, P., Hu, Y., & Cheng, H. (2019). Municipal Solid Waste (MSW) Incineration Fly Ash as an Important Source of Heavy Metal Pollution in China. Environmental Pollution, 252, 461–475. https://doi.org/10.1016/j.envpol.2019.04.082

Wungsumpow C, Towprayoon S, Chiemchaisri C, Suanburi D, Wangyao K (2018). Applying Electrical Resistivity Tomography Measurement in Landfill Mining: A Study on Configuration and Spacing Setting. 7th SEE 2018: Technology and innovation for global energy revolution, Bangkok, Thailand.

Xiao, H., & Liu, Y. (2018). A Prediction Model for the Tensile Strength of Cement-Admixed Clay with Randomly Orientated Fibres. European Journal of Environmental and Civil Engineering, 22(9), 1131–1145.

Yingsamphancharoen, T., & Piriyakul, K. (2022). Feasibility Study of Steel Reinforcement of Polyethylene Corrugated Horizontal Pipe for On-Site Underground Water Storage Tanks and Their Applications. *Case Studies in Construction Materials*, *17*, e01578.

Zak, P., Ashour, T., Korjenic, A., Korjenic, S., & Wu, W. (2016). The Influence of Natural Reinforcement Fibers, Gypsum and Cement on Compressive Strength of Earth Bricks Materials. Construction and Building Materials, 106, 179-188.